

## Original Research



# Kaempferol ameliorates metabolic syndrome by inhibiting inflammation and oxidative stress in high-fat diet-induced obese mice

Su-Kyung Shin <sup>1,2</sup>, and Eun-Young Kwon <sup>1,2,3§</sup>

<sup>1</sup>Department of Food Science and Nutrition, Kyungpook National University, Daegu 41566, Korea

<sup>2</sup>Center for Food and Nutritional Genomics Research, Kyungpook National University, Daegu 41566, Korea

<sup>3</sup>Center for Beautiful Aging, Kyungpook National University, Daegu 41566, Korea



Received: Mar 11, 2024

Revised: Apr 6, 2024

Accepted: Apr 11, 2024

Published online: Apr 22, 2024

### §Corresponding Author:

Eun-Young Kwon

Department of Food Science and Nutrition,  
Kyungpook National University, 80 Daehak-ro,  
Buk-gu, Daegu 41566, Korea.

Tel. +82-53-950-6231

Fax. +82-53-950-6229


Email. eykwon@knu.ac.kr

©2024 The Korean Nutrition Society and the Korean Society of Community Nutrition  
This is an Open Access article distributed under the terms of the Creative Commons Attribution Non-Commercial License (<https://creativecommons.org/licenses/by-nc/4.0/>) which permits unrestricted non-commercial use, distribution, and reproduction in any medium, provided the original work is properly cited.

### ORCID iDs

Su-Kyung Shin 

<https://orcid.org/0000-0002-8918-3995>

Eun-Young Kwon 

<https://orcid.org/0000-0001-8357-9158>

### Funding

This work was supported by the National Research Foundation of Korea (NRF) grant funded by the Korea government (MSIT) (No. RS-2023-00237118 and No. 2021R1A2C1011233).

## ABSTRACT

**BACKGROUND/OBJECTIVES:** Kaempferol (Ka) is one of the most widely occurring flavonoids found in large amounts in various plants. Ka has anti-obesity, antioxidant, and anti-inflammatory effects. Despite the numerous papers documenting the efficacy of Ka, some controversy remains. Therefore, this study examined the impact of Ka using 3T3-L1 and high-fat diet-induced obese mice.

**MATERIALS/METHODS:** 3T3-L1 cells were treated with 50  $\mu$ M Ka from the initiation of 3T3-L1 differentiation at D0 until the completion of differentiation on D8. Thirty male mice (C57BL/6J, 4 weeks old) were divided into 3 groups: normal diet (ND), high-fat diet (HFD), and HFD + 0.02% (w/w) Ka (Ka) group. All mice were fed their respective diets *ad libitum* for 16 weeks. The mice were sacrificed, and the plasma and hepatic lipid levels, white adipose tissue weight, hepatic glucose level, lipid level, and antioxidant enzyme activities were analyzed, and immunohistochemistry staining was performed.

**RESULTS:** Ka suppressed the hypertrophy of 3T3-L1 cells, and the Ka-supplemented mice showed a significant decrease in perirenal, retroperitoneal, mesenteric, and subcutaneous fat compared to the HFD group. Ka supplementation in high-fat diet-induced obese mice also improved the overall blood lipid concentration (total cholesterol, non-high-density lipoprotein-cholesterol, phospholipids, and apolipoprotein B). Ka supplementation in high-fat-induced obesity mice reduced hepatic steatosis and insulin resistance by modulating the hepatic lipid (glucose-6-phosphate dehydrogenase, fatty acid synthase, malic enzyme, phosphatidate phosphohydrolase, and  $\beta$ -oxidation) activities and glucose (glucokinase, phosphoenolpyruvate carboxykinase, and G6pase)-regulating enzymes. Ka supplementation ameliorated the erythrocyte and hepatic mitochondrial H<sub>2</sub>O<sub>2</sub> and inflammation levels (plasma tumor necrosis factor- $\alpha$ , monocyte chemoattractant protein-1, interleukin-6, and interferon- $\gamma$  and fibrosis of liver and epididymal fat).

**CONCLUSION:** Ka may be beneficial for preventing diet-induced obesity, inflammation, oxidative stress, and diabetes.

**Keywords:** Obesity; inflammation; oxidative stress; fatty liver; metabolic syndrome

### Conflict of Interest

The authors declare no potential conflicts of interests.

### Author Contributions

Formal analysis: Shin SK; Investigation: Kwon EY; Supervision: Kwon EY; Writing - original draft: Shin SK; Writing - review & editing: Shin SK.

## INTRODUCTION

Obesity is characterized by an increase in the number and size of adipocytes, with expansion occurring when energy intake exceeds expenditure. Approximately 30% of the world's population is considered obese. Obesity has emerged as a significant social concern owing to its close association with heightened mortality and morbidity rates [1].

Obesity is closely linked to chronic inflammation within the body. This obesity-triggered inflammatory reaction is a significant contributor to metabolic syndrome. Previously, adipose tissue was viewed merely as a passive depot for storing excess energy in the form of neutral fat, which could be mobilized into free fatty acids (FFAs) for energy when needed. Recently, however, it has been reported to produce various adipokines, such as adiponectin, leptin, resistin, tumor necrosis factor- $\alpha$  (TNF $\alpha$ ), adiponin, plasminogen activator inhibitor-1 (PAI-1), glucose-dependent insulinotropic polypeptide (GIP), monocyte chemoattractant protein-1 (MCP-1), interferon- $\gamma$  (IFN- $\gamma$ ), interleukin (IL)-6, and IL-10, as well as vasoactive substances in white adipose tissue (WAT) [2-4]. These substances are involved in energy requirements, appetite regulation, insulin sensitivity, cardiovascular disease, immunity, and inflammatory responses [5]. The primary feature of the inflammatory response involves the infiltration of immune cells, including neutrophils, eosinophils, and macrophages, into the inflamed tissue. The proliferation of adipocytes and their enlargement attract macrophages, which produce inflammatory cytokines and chemokines such as leptin, resistin, TNF $\alpha$ , PAI-1, MCP-1, and IL-6 [6].

The excessive production of reactive oxygen species (ROS) by obesity has been consistently shown in experimental and clinical cases [7]. Insulin resistance is the most common feature in obese patients and is accompanied by an increase in ROS and inflammatory mediators [8]. Specifically, increased oxidative stress caused by obesity is associated with insulin resistance,  $\beta$ -cell dysfunction, impaired glucose tolerance, and ultimately, the development of type 2 diabetes [9,10]. Hyperglycemia induces inflammation and elevates oxidative stress markers, leading to vascular dysfunction. Hence, the most significant contribution to oxidative stress in the metabolic syndrome process is related to the components associated with obesity and insulin resistance [11]. These discoveries highlight the link between obesity, inflammation, oxidative stress, and insulin resistance, underscoring the necessity for interventions that address these intertwined pathways to tackle metabolic dysfunctions.

Kaempferol (Ka) is one of the most widely occurring flavonoids found in large amounts in various plants, including tea, cruciferous vegetables, grapefruit, ginkgo biloba, and some edible fruits [12,13]. Ka has been reported to have anti-obesity efficacy, such as increasing energy expenditure in human skeletal muscle and reducing plasma triglycerides (TG) and body weight when administered to rats [14,15]. Moreover, the treatment of pancreatic  $\beta$ -cells and MC3T3-E1 osteoblastic cells with Ka resulted in decreased oxidative damage [16,17]. The administration of Ka to the cytokine-induced pro-inflammatory status of human endothelial cells and activated macrophages inhibited the inflammatory responses [18,19]. Although Ka has been reported to have anti-obesity, antioxidant, and anti-inflammatory effects, Ninomiya *et al.* [20] reported that the administration of Ka tended to decrease body weight and visceral fat mass, but the change was not statistically significant. In addition, Christensen *et al.* [21] reported that Ka administration is ineffective in the lipid and glucose metabolism.

Despite numerous papers documenting the efficacy of Ka, some controversy remains. Therefore, this study examined the impact of Ka on 3T3-L1 cell differentiation to determine

the potential anti-obesity effects. In addition, the efficacy of Ka on the inflammation and insulin resistance closely associated with obesity was evaluated using high-fat diet-induced obese mice.

## MATERIALS AND METHODS

### Cell culture and Ka treatment

3T3-L1 cells (passage 5–8) were cultured in Dulbecco's Modified Eagle Medium (DMEM) supplemented with 10% (v/v) calf serum and 1% (v/v) penicillin/streptomycin (Thermo Fisher Scientific, Waltham, MA, USA) at 37°C in a humidified 5% CO<sub>2</sub> atmosphere. Differentiation was induced by providing the 48 h post-confluent 3T3-L1 cells with DMEM supplemented with 10% fetal bovine serum (FBS), 1 µg/mL insulin, 0.5 mM 3-iso-butyl-1-methylxanthine, and 1 µM dexamethasone. The cells were cultured in DMEM supplemented with 10% (v/v) FBS and 1 µg/mL insulin for 2 days. For further cell culture, the medium was replaced with DMEM supplemented with 10% (v/v) FBS every 2 days. Ka was purchased from Sigma-Aldrich Co., Ltd. (St. Louis, MO, USA).

The cells were treated with 50 µM Ka from the initiation of cell differentiation on D0 until the completion of differentiation on D8. All experiments were performed in duplicate and repeated at least 3 times to ensure reproducibility.

### Cell viability assay

The cell viability was measured using the colorimetric 3-(4,5)di-methylthiazol-2-yl)-2,5-diphenyltetrazolium bromide (MTT) assay method. Living cells reduced MTT to formazan, which was quantified by measuring the absorbance at 570 nm. The cells were grown to confluence in 96-well plates and incubated with 0.1% DMSO or 10–150 µM Ka for 24–72 h. The control cells were prepared in plates containing only medium. At the end of the incubation period, MTT was added to each well, and incubation was carried out for 4 h at 37°C. Formazan production is expressed as a percentage of the values obtained from the control cells.

### Oil Red O (ORO) staining of 3T3-L1 cells

The 3T3-L1 cells were rinsed with PBS, fixed in 10% formalin at 37°C and 5% CO<sub>2</sub>, washed with 60% isopropanol, stained with ORO solution (Sigma-Aldrich Co., Ltd.) for 15 min at 25°C, and rinsed with PBS to remove the unattached ORO. The stained cells were imaged using a DM-IL microscope (Leica, Wetzlar, Germany) at 400× magnification and extracted using 100% isopropanol to quantify lipid accumulation. Isopropanol from an empty well was used as a control, and the absorbance was measured spectrophotometrically at 510 nm to quantify ORO staining.

### Animals and diet

Thirty male mice (C57BL/6J, 4 weeks old) were obtained from Jackson Laboratory. All mice were housed under controlled conditions (12-h light-dark cycle, 25°C, 40–60% humidity) and underwent an acclimatization period. The mice were then sorted into 3 groups: normal diet (ND) group (n = 10, 11% kcal from fat), high-fat diet (HFD) group (n = 10, 40% kcal from fat), and HFD + 0.02% (w/w) Ka (Ka) group (n = 10). Each group was provided their respective diets *ad libitum* for 16 weeks. **Table 1** lists the composition of the diets used in the experiment. The animal experiment procedures complied with the protocols approved by the Kyungpook National University Ethics Committee (Approval No. KNU 2010-4-14).

**Table 1.** Diet composition for the animal experiment

Ingredient (g)	ND	HFD	HFD + Ka
Casein	200.00	200.00	200.00
D, L-methionine	3.00	3.00	3.00
Corn starch	150.00	111.00	111.00
Sucrose	500.00	370.00	369.98
Cellulose powder	50.00	50.00	50.00
Corn oil	50.00	30.00	30.00
Lard	-	170.00	170.00
Mineral mixture <sup>1)</sup>	35.00	42.00	42.00
Vitamin mixture <sup>2)</sup>	10.00	12.00	12.00
Choline bitartrate	2.00	2.00	2.00
Cholesterol	-	10.00	10.00
Tert-butylhydroquinone	0.01	0.04	0.04
Kaempferol	-	-	0.02
Total (g)	1,000	1,000	1,000
Total energy (kcal)	3,850	4,524	4,524

ND, normal diet group; HFD, high-fat diet group; HFD + Ka, high-fat diet + 0.02% kaempferol group. <sup>1)</sup>AIN-76 mineral mixture (grams/kg): calcium phosphate, 500; sodium chloride, 74; potassium citrate, 2220; potassium sulfate, 52; magnesium oxide, 24; manganous carbonate, 3.5; ferric citrate, 6; zinc carbonate, 1.6; cupric carbonate, 0.3; potassium iodate, 0.01; sodium celenite, 0.01; chromium potassium sulfate, 0.55; sucrose 118.03. <sup>2)</sup>AIN-76 vitamin mixture (grams/kg): thiamin HCl, 0.6; riboflavin, 0.6; pyridoxine HCl, 0.7; nicotinic acid, 0.003; D-calcium pantothenate, 0.0016; folate, 0.2; D-biotin, 0.02; cyanocobalamin (vitamin B12), 0.001; retinyl palmitate premix, 0.8; DL-alpha tocopheryl acetate, premix, 20; cholecalciferol (vitamin D3), 0.0025; menaquinone (vitamin K), 0.05; antioxidant, 0.01; sucrose, finely powdered, 972.8.

### Sample preparation

Upon completion of the experimental period, all mice were fasted for 12 h and euthanized using isoflurane (5 mg/kg body weight; Urim Pharm, Daejeon, Korea). Blood samples were collected via the inferior vena cava and placed into heparin-coated tubes for subsequent biomarker analysis. The collected blood samples underwent centrifugation at  $1,000 \times g$  for 15 min at 4°C to separate the plasma, which was then stored in a deep freezer. The liver and adipose tissue were excised swiftly, rinsed with physiological saline, and weighed. The excised tissues were promptly flash-frozen in liquid nitrogen and preserved at -70°C.

### Lipid profiles in plasma and tissues

The plasma total cholesterol (TC), TG, high-density lipoprotein cholesterol (HDL-C), and phospholipids levels were assessed using enzyme kits from Asan Pharm Co., Seoul, Korea. In addition, the plasma-FFA levels were determined using kits from Wako Chemicals, Osaka, Japan. The apolipoprotein (apo) A1 (apoA1) and apoB100 levels were measured using kits from Eiken Chemical Co., Tokyo, Japan. The non-HDL-C value, HDL-C-to-TC ratio (HTR), and atherogenic index (AI) were calculated as follows: Non-HDL-C = TC - HDL-C - (TG/5); HTR (%) = (HDL-C/TC) × 100; and AI = (TC - HDL-C)/HDL-C.

For liver lipid extraction, the dried lipid residues were dissolved in 1 mL of ethanol. Emulsification was facilitated by adding 200 μL of an emulsifier containing Triton X-100 and sodium cholate in distilled water to the dissolved lipid solution. Cholesterol, TG, and fatty acids (FAs) were then measured using the same enzyme kit used for plasma analysis.

### Plasma cytokines and inflammatory factors

The plasma concentrations of adiponectin, leptin, resistin, adipsin, PAI-1, GIP, TNFα, MCP-1, IL-6, and interferon-γ (IFN-γ) were assessed using a multiplex detection kit sourced from Bio-Rad, Millipore, located in Hercules, CA, USA.

### Plasma glucose, insulin, glucagon, homeostatic model assessment of insulin resistance (HOMA-IR) index, and intraperitoneal glucose tolerance test (IPGTT)

The plasma glucose levels were determined using the glucose assay kit from Abcam (Cambridge, UK), while the insulin levels were measured using the Mouse Insulin ELISA Kit from Thermo Fisher Scientific. The plasma glucagon levels were assessed using a Glucagon Immunoassay Quantikine ELISA Kit from R&D Systems, located in Minneapolis, MN, USA. The HOMA-IR index was calculated using the formula: (Fasting Insulin Concentration (mU/L) × Fasting Glucose Concentration (mg/dL) × 0.05551)/22.5. For the IPGTT, conducted 14 weeks after the commencement of the experiment, the mice were fasted for 12 h and injected intraperitoneally with glucose (0.5 g/kg body weight). The blood glucose levels were then measured from the tail vein at 0, 30, 60, and 120 min post-injection.

### Hepatic glycogen level

The glycogen concentration was assessed with minor adaptations of the method outlined by Carroll *et al.* [22] in 1956. For liver glycogen determination, 80  $\mu$ L of 30% KOH was introduced post-tissue extraction. After heating at 100°C for 30 min, 200  $\mu$ L of 95% ethanol was introduced, and the mixture was left to incubate overnight at 4°C. The resulting pellet obtained through centrifugation was dissolved in 1 mL of distilled water. Anthrone reagent was then added and heated to 100°C for 20 min, and the glycogen concentration was quantified based on the absorbance at 620 nm.

### Glucose-related enzyme activity analysis in the liver

The glucokinase activity in the cytosol was evaluated using a spectrophotometric assay reported by Davidson and Arion [23]. The phosphoenolpyruvate carboxykinase (PEPCK) activity was determined by measuring the rate of oxaloacetate synthesis and the reduction of NADH to NAD, according to the spectrophotometric protocol established by Bentle and Lardy [24]. The G-6-pase activity was assessed using a slight modification of the method reported by Alegre *et al.* [25].

### Lipid-regulated enzyme activities in the liver

The activity of fatty acid synthase (FAS) in the cytosol was determined using the procedure outlined by Nepokroeff *et al.* [26]. The ME activity was evaluated by measuring NADPH production in the cytosol. The assay was initiated by adding 600  $\mu$ L of 0.4 M triethanolamine buffer to the tube, followed by the sequential addition of reagents: 30 nM L-malate, 0.12 M MnCl<sub>2</sub>, and 3.4 nM TPN. The absorbance was recorded at 340 nm. Glucose-6-phosphate dehydrogenase (G6PD) activity was determined by assessing the extent of NADP<sup>+</sup> reduction to NADPH [27]. The phosphatidate phosphohydrolase (PAP) activity was measured in microsomes, where Reagent A (0.05 M Tris-HCl, 1.25 mM EDTA, and 1 mM MgCl) and Reagent B (1.8 M H<sub>2</sub>SO<sub>4</sub>, SDS, and ascorbic acid) were added, and absorbance was measured at 820 nm. The carnitine palmitoyltransferase activity in the mitochondria was analyzed using the protocol outlined by Markwell *et al.* [28].  $\beta$ -oxidation activity was assessed by quantifying the reduction of NAD<sup>+</sup> to NADH using palmitoyl-coenzyme A (CoA) as a substrate, according to Lazarow's method [29].

### Hepatic 3-hydroxy-3-methylglutaryl coenzyme A (HMG-CoA) reductase (HMGR) and acyl-coenzyme A:cholesterol acyltransferase (ACAT) activities

The microsomal HMGR activities were assessed with [14C]-HMG-CoA as the substrate using a slight modification of the method introduced by Shapiro *et al.* [30]. The micromic ACAT

activities were determined using [14C]-oleoyl CoA according to the procedure outlined by Gillies *et al.* [31].

### Hydrogen peroxide and thiobarbituric acid reactive substances (TBARS)

The hydrogen peroxide levels were evaluated using Wolff's method, with absorbance measurements recorded at 560 nm. The TBARS content was quantified according to the protocol described by Ohkawa, with the absorbance readings of the supernatant taken at 532 nm after centrifugation [32].

### Antioxidant enzyme activity analysis

The superoxide dismutase (SOD) activity was assessed using the autoxidized pyrogallol reagent according to the procedure outlined by Marklund and Marklund [33]. The catalase (CAT) enzyme activity, responsible for the decomposition of H<sub>2</sub>O<sub>2</sub> into H<sub>2</sub>O and O<sub>2</sub>, was determined using the methodology established by Aebi [34]. The glutathione peroxidase (GSH-Px) activity was measured with minor adjustments to the method devised by Paglia and Valentine [35].

### Real-time quantitative polymerase chain reaction analysis

The total RNA was extracted from 3T3-L1 cells. Reverse transcription was conducted to convert the RNA samples into cDNA. The resulting cDNA samples were then diluted with DEPC, and mRNA expression analysis was carried out using TB Green® Premix EX TaqTMII on a CFX96TM Real-Time Detection System (Bio-Rad). **Table 2** lists the primers for the target genes. The cycle threshold values were normalized using GAPDH as an internal reference.

### Histological and immunohistochemistry analysis

The liver and WAT extracted from the mice were fixed using a 10% formalin solution buffer. The fixed samples were then embedded in paraffin, cut into 5 µm-thick sections, and stained with hematoxylin and eosin as well as Masson's trichrome (MT). For immunohistochemistry analysis, the islets were sectioned, fixed in H<sub>2</sub>O<sub>2</sub>, and rinsed in citrate buffer (pH 6.0). The sections were then treated with a blocking reagent (Ultra Tech HRP; Beckman Coulter, Brea, CA, USA) to minimize nonspecific binding and incubated with monoclonal antibodies targeting insulin and glucagon (Santa Cruz Biotech Inc., Dallas, TX, USA). The antibody reactivity was detected using horseradish peroxidase-conjugated biotin-streptavidin

**Table 2.** Primer sequences for real-time polymerase chain reaction

Primer	Sequence (5'-3')
GAPDH	F: TGC AGT GGC AAA GTG GAG AT R: TTG AAT TTG CCG TGA GTG GA
PPAR $\gamma$	F: ATG CCA AAA ATA TCC CTG GTT TC R: GGA GGC CAG CAT CGT GTA GA
FAS	F: GCT GCG GAA ACT TCA GGA AAT R: AGA GAC GTG TCA CTC CTG GAC TT
Leptin	F: GCA GTG CCT ATC CAG AAA GTC C R: GGA ATG AAG TCC AAG CCA GTG AC
TNF $\alpha$	F: AAA GAC ACC ATG AGC ACA GAA AGC R: GCC ACA AGC AGG AAT GAG AAG AG
Cd44	F: GAA TGTAACCT CCGCTACG R: GGAGGTGTTGGACGTGAC
MCP-1	F: TTC CTC CAC CAC CAT GCA G R: CCA GCC GGC AAC TGT GA

GAPDH, glyceraldehyde 3-phosphate dehydrogenase; PPAR $\gamma$ , peroxisome proliferator-activated receptor gamma; FAS, fatty acid synthase; TNF $\alpha$ , tumor necrosis factor-alpha; Cd44, CD44 molecules; MCP-1, monocyte chemoattractant protein-1.

complexes and developed with diaminobenzidine tetrahydrochloride as the substrate. The stained areas were visualized under an optical microscope with a magnification of  $\times 200$ . Similar procedures were performed for the liver and WAT samples, where MCP-1 and Cd68 polyclonal antibodies were diluted at 1:50, reacted, developed with New fuchsin, and observed under a microscope at  $\times 400$  magnification. The stained tissues were examined using an optical microscope (Zeiss Axio Scope; Zeiss, Oberkochen, Germany).

### Microarray analysis

The total RNA underwent amplification and purification using the Ambion Illumina RNA amplification kit (Ambion, Waltham, MA, USA). Biotinylated cRNA (750 ng per sample) was then hybridized onto Illumina MouseWG-6 v2 Expression BeadChips (Illumina, San Diego, CA, USA) according to the manufacturer's instructions. After hybridization, arrays underwent washing and staining with Amersham Fluorolink streptavidin-Cy3 (GE Healthcare Bio-Sciences, Little Chalfont, UK) according to the standard protocol outlined in the bead array manual. The hybridization quality and overall chip performance were evaluated by visually inspecting the internal quality controls and raw scanned data in Illumina BeadStudio software. The probe signal intensities were quantile-normalized and log-transformed. Differential gene expression between the groups was analyzed using the non-parametric RankProd approach. Oligonucleotides demonstrating changes with a false discovery rate  $< 0.05$  between groups were considered statistically significant.

### Statistical analysis

The data were analyzed using the SPSS software package (IBM SPSS Statistics, Chicago, IL, USA). The experimental results are expressed as the mean  $\pm$  SE of the mean. A Student's *t*-test was used to compare the CON and Ka 50  $\mu\text{M}$  or ND and HFD groups with the following significance levels: \* $P < 0.05$ , \*\* $P < 0.01$ , \*\*\* $P < 0.001$ . Similarly, comparisons between the HFD group and Ka groups were conducted using a Student's *t*-test with the following significance levels: # $P < 0.05$ , ## $P < 0.01$ , ### $P < 0.001$ .

## RESULTS

### Ka suppressed hypertrophy of 3T3-L1 cells

The anti-obesity efficacy of Ka was verified by first analyzing the effect of Ka on adipocyte differentiation using 3T3-L1 cells. Ka cytotoxicity against 3T3-L1 cells was determined using an MTT assay. The cell viability was affected by Ka in a time- and dose-dependent manner. The cell viability was less than 70% when the cells were treated with Ka concentrations above 75  $\mu\text{M}$  for 24 h. On the other hand, Ka concentrations equal to or below 50  $\mu\text{M}$  were safely tolerated by the cells for up to 72 h. Therefore, 50  $\mu\text{M}$  was the highest concentration for further experiments (**Fig. 1A**). The 3T3-L1 cells were incubated in adipogenic differentiation medium in the presence of 50  $\mu\text{M}$  Ka for 8 days, resulting in the inhibition of adipocyte differentiation. The resulting decrease in lipid accumulation after exposure to 50  $\mu\text{M}$  Ka was observed using ORO staining (**Fig. 1B**). This effect was observed 48 h after treatment with Ka 50  $\mu\text{M}$ . On the eighth day, fat accumulation was suppressed by more than 40% compared to the CON group. Among several highly expressed genes in mature adipocytes, the gene expression of PPAR $\gamma$ , FAS, and leptin measured at D8 was significantly lower in the Ka 50  $\mu\text{M}$  group than the CON group (**Fig. 1C**). The excessive proliferation of adipocytes causes inflammation. Ka significantly reduced the mRNA expression of *Mcp-1* and slightly decreased the mRNA expression of *TNF $\alpha$*  and *Cd44* compared to the CON group (**Fig. 1D**). Hence, the anti-obesity

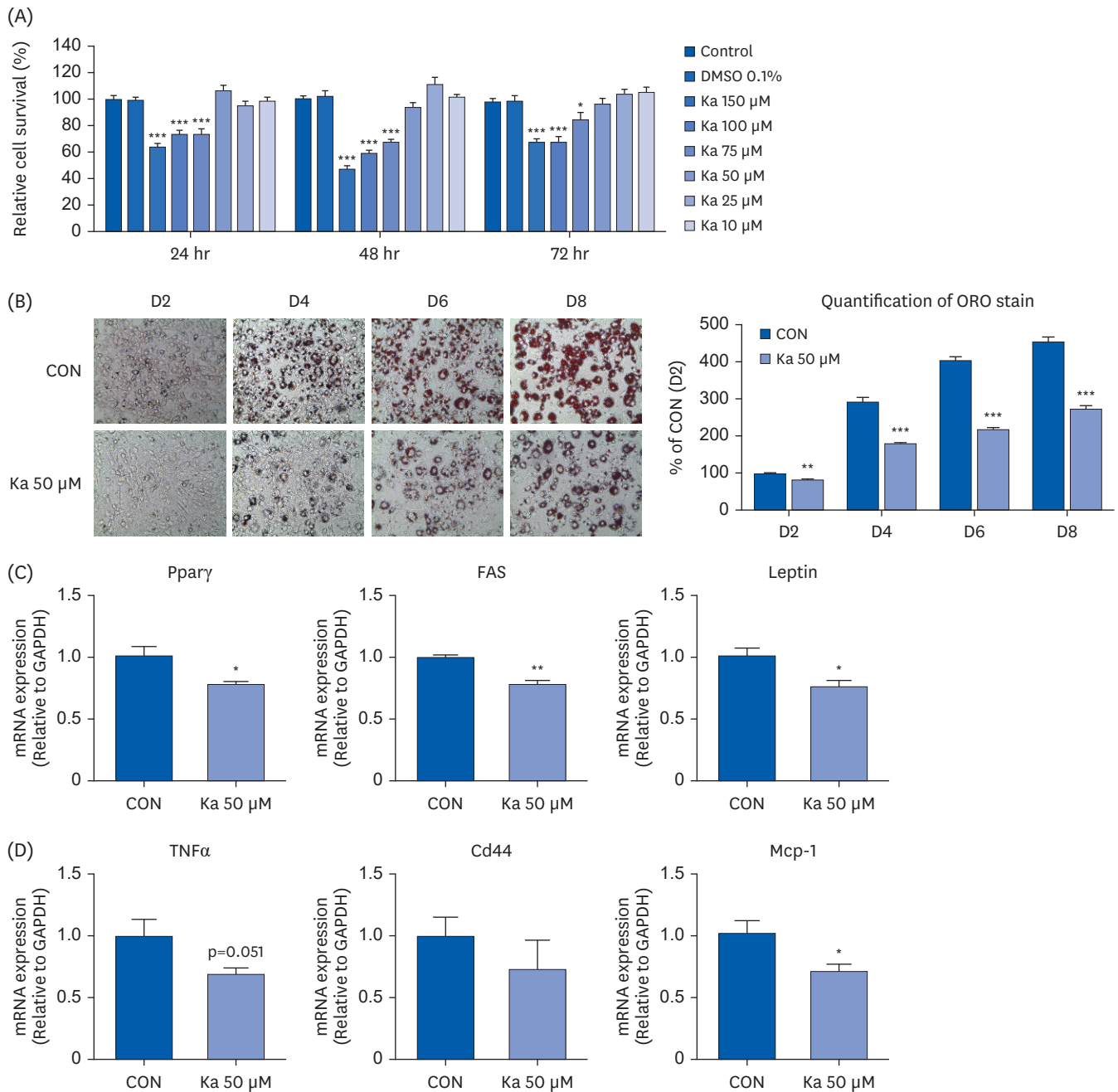


**Fig. 1.** Effects of Ka on the cell viability of 3T3-L1 cells (A), ORO staining of 3T3-L1 cells treated with Ka 50 μM (B), mRNA expression of lipogenesis of 3T3-L1 cells treated with Ka 50 μM (C), mRNA expression of the inflammatory factors of 3T3-L1 cells treated with Ka 50 μM (D). Data are expressed as the mean ± SE of the mean. DMSO, dimethyl sulfoxide; Ka, kaempferol; ORO, Oil Red O; Pparγ, peroxisome proliferator activated receptor gamma; FAS, fatty acid synthase; TNFα, tumor necrosis factor-alpha; Cd44, CD44 molecules; Mcp-1, monocyte chemoattractant protein-1. Student's *t*-test, *n* = 3, \**P* < 0.05, \*\**P* < 0.01, \*\*\**P* < 0.001 vs. DMSO 0.1% (CON).

effect of Ka was confirmed in 3T3-L1 cells. Therefore, further experiments were conducted to determine if it would have the same effect by supplementing high-fat diet-induced obese mice with Ka.



**Ka supplementation reduced adiposity and plasma lipid profiles**

**Fig. 2A** shows the average weight change during 16 weeks of feeding the experimental diet. Overall, the average body weight of all groups tended to increase gradually during the experiment period. From the second week of the experiment, the body weight was significantly higher in the HFD group than in the ND group. From the sixth week, the Ka group had a significantly lower body weight than the HFD group.

During the experimental period, the average dietary intake of the HFD group was significantly lower than that of the ND group; the dietary intake was similar in the Ka and HFD groups (**Fig. 2B**). When comparing the weight gain according to dietary intake, the HFD group showed significantly higher weight gain than the ND group, and the Ka-supplemented group showed a decrease.

The weight of WAT according to various regions was compared. The weight of all WAT in the HFD group mice increased significantly compared to the ND group, indicating that obesity induction using a high-fat diet was successful. The perirenal, mesenteric, retroperitoneum, and subcutaneous fat were significantly lower in the ND group than in the HFD group due to Ka administration, resulting in a significantly lower total WAT (**Fig. 2C**). **Fig. 2D** shows the morphological changes of WAT in the ND, HFD, and Ka-supplemented group. The size of the adipocytes in the HFD group increased due to high-fat diet consumption, and Ka supplementation significantly reduced the size of adipocytes compared to the HFD group. **Fig. 2E** shows the plasma lipid concentration obtained by sacrificing 16 weeks after feeding

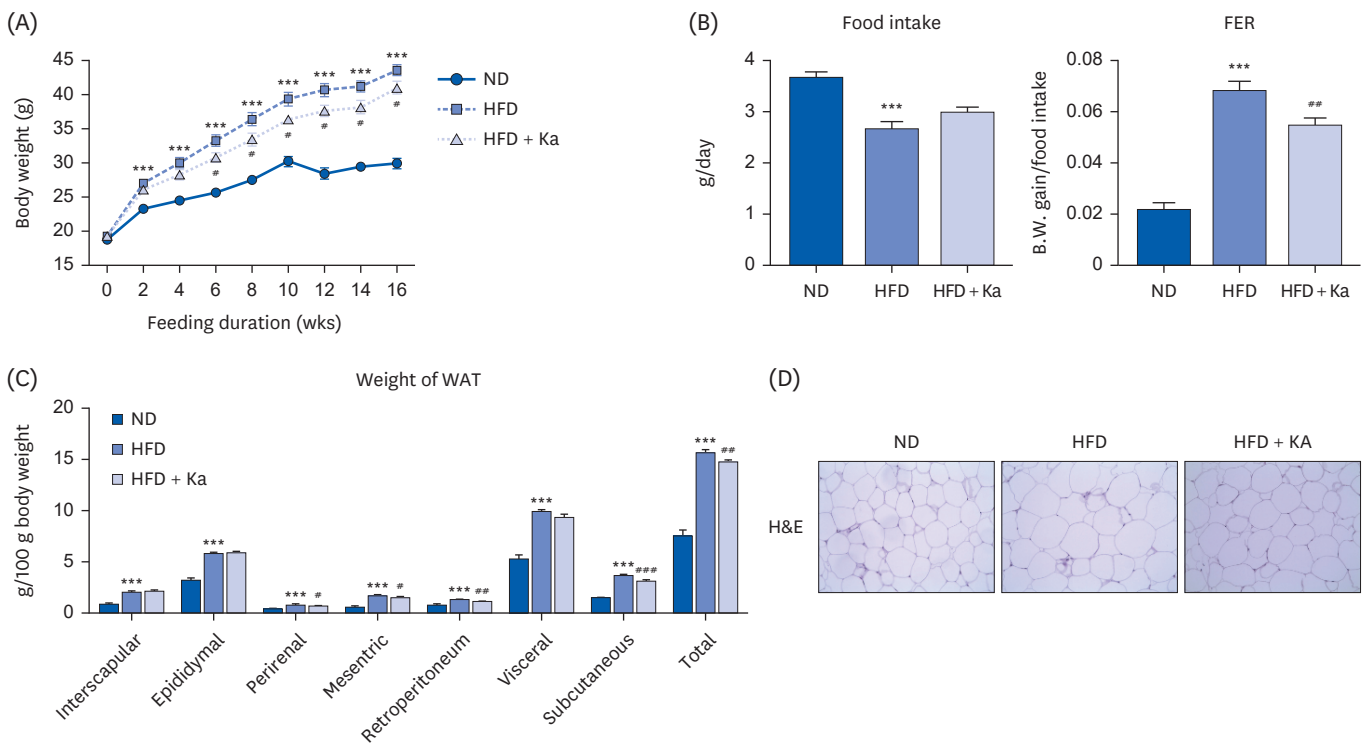


**Fig. 2.** Effects of Ka on body weight (A), food intake; FER (B), WAT weight (C), representative images for H&E staining of epididymal WAT (D), plasma lipid profiles (E) in C57BL/6J mice fed a HFD; The data are expressed as the mean ± SE of the mean. ND, normal diet (AIN-76); Ka, kaempferol; HFD, high-fat diet; HFD + Ka, high-fat diet + 0.02% kaempferol; FER, food efficiency ratio; WAT, white adipose tissue; H&E, hematoxylin and eosin; TC, total cholesterol; HDL-C, high-density lipoprotein cholesterol; HTR, high-density lipoprotein cholesterol/total cholesterol ratio; TG, triglycerides; FFA, free fatty acid; Apo, apolipoprotein; RBC, red blood cell; TBARS, thiobarbituric acid reactive substances. Student's t-test, \**P* < 0.05, \*\*\**P* < 0.001 vs. ND; #*P* < 0.05, ###*P* < 0.001 vs. HFD.

(continued to the next page)

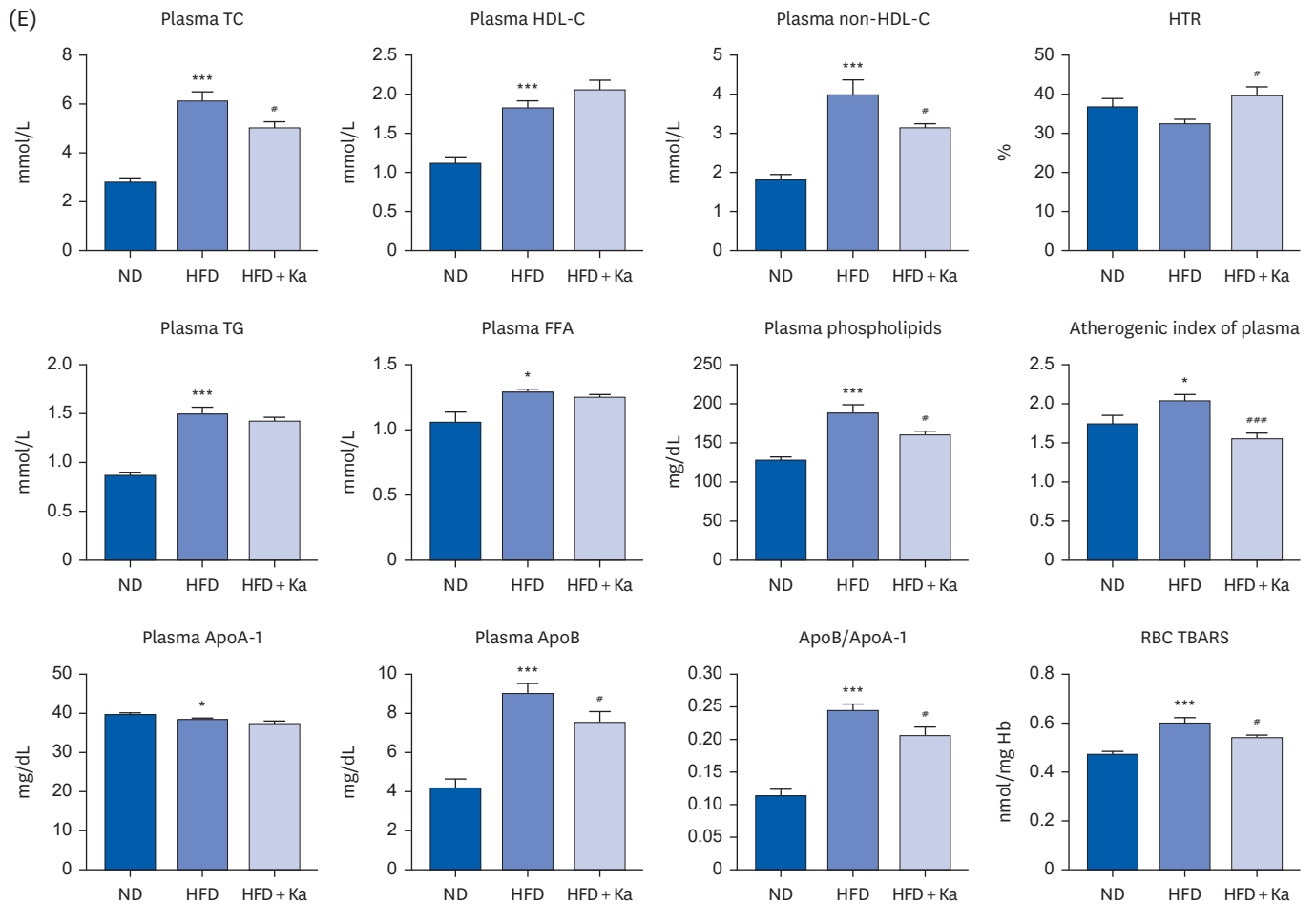


**Fig. 2.** (Continued) Effects of Ka on body weight (A), food intake; FER (B), WAT weight (C), representative images for H&E staining of epididymal WAT (D), plasma lipid profiles (E) in C57BL/6J mice fed a HFD; The data are expressed as the mean  $\pm$  SE of the mean. ND, normal diet (AIN-76); Ka, kaempferol; HFD, high-fat diet; HFD + Ka, high-fat diet + 0.02% kaempferol; FER, food efficiency ratio; WAT, white adipose tissue; H&E, hematoxylin and eosin; TC, total cholesterol; HDL-C, high-density lipoprotein cholesterol; HTR, high-density lipoprotein cholesterol/total cholesterol ratio; TG, triglycerides; FFA, free fatty acid; Apo, apolipoprotein; RBC, red blood cell; TBARS, thiobarbituric acid reactive substances. Student's *t*-test, \**P* < 0.05, \*\*\**P* < 0.001 vs. ND; #*P* < 0.05, \*\*\**P* < 0.001 vs. HFD.

the experimental diet. Except for ApoA, all plasma lipid concentrations in the ND group were significantly lower than those in the HFD group. The TC and non-HDL-C were significantly lower in the Ka group than in the HFD group. The HTR (%), the HDL-C to TC ratio, was significantly higher in the Ka group than in the HFD group. The plasma phospholipid and AI levels, which are the arteriosclerosis index, were also significantly lower in the Ka group than in the HFD. The plasma ApoA-1 level in the Ka group was not significantly different from the HFD group, whereas the Apo B level was significantly lower in the Ka group. As a result, the ApoB/ApoA-1 ratio, a biomarker for predicting arteriosclerosis and cardiovascular disease, was significantly lower in the Ka group than in the HFD group. The TBARS levels indicated that the peroxidation of red blood cells (RBCs) was significantly higher in the HFD group than in the ND group and significantly lower in the Ka group than in the HFD group (**Fig. 2E**). Based on the above experimental results, Ka supplementation in the high-fat diet-induced obesity mice is believed to reduce adiposity and improve the overall blood lipid concentration.

### Ka supplementation reduced hepatic steatosis and insulin resistance

Ka also significantly reduced the liver weight and the accumulation and size of hepatic lipid droplets relative to that of mice in the HFD group (**Fig. 3A and B**). Furthermore, Ka supplementation markedly decreased the hepatic TG, fatty acid (FA), and cholesterol contents compared to that of mice in the HFD group (**Fig. 3C**). The activities of the hepatic enzymes involved in lipogenesis (G6PD, FAS, ME, and PAP) were reduced significantly. Those related to FA oxidation and  $\beta$ -oxidation were increased markedly by the Ka treatment compared to those in mice in the HFD group (**Fig. 3D**). The activities of the hepatic cholesterol-regulating enzymes 3-hydroxy-3-methyl-glutaryl-CoA reductase and ACAT were also remarkably lower in the mice in the Ka group than those in the HFD group (**Fig. 3E**). The hepatic TBARS levels were significantly higher in the HFD group than in the ND group, and significantly lower in the Ka group than in the HFD group, which is consistent with the patterns observed in RBC TBARS levels (**Fig. 3F**).

Ka supplementation significantly decreased the plasma glucose, insulin, and glucagon levels, and HOMA-IR index compared to that in the mice in the HFD group (**Fig. 4A**). The striking improvement of hepatic steatosis coupled with the decreased adiposity in the Ka supplemented mice was associated with a normalization of the plasma glucose and insulin levels, which was a reflection of improved hepatic insulin sensitivity, as evidenced by the IPGTT and reduced area under curve (**Fig. 4B**). The glycogen levels and glucokinase, PEPCK, and G6Pase activities were lowered by UR compared to those in the livers of mice in the HFD group (**Fig. 4C**). Immunohistochemical staining of the pancreatic tissue for insulin and glucagon also showed that Ka supplementation prevented pancreatic islet hypertrophy caused by a HFD, normalizing the insulin and glucagon content in the plasma (**Fig. 4D**).

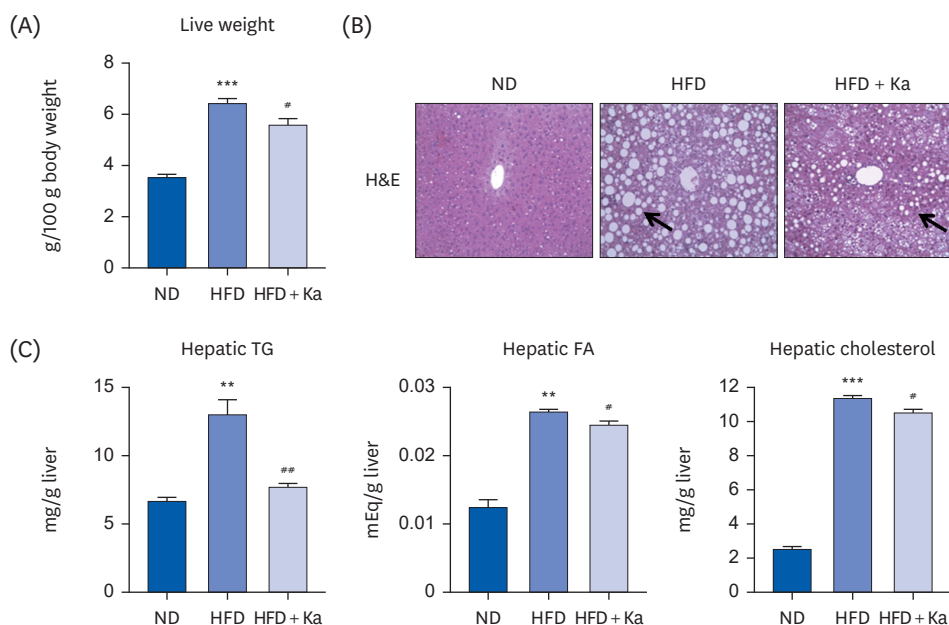


**Fig. 3.** Effects of Ka on the liver weight (A), representative images of H&E staining of the liver (B), hepatic lipid profiles (C), hepatic lipid-regulating enzyme activities (D), hepatic cholesterol-regulating enzyme activities (E), and hepatic TBARS (F) in C57BL/6J mice fed a HFD; the data are expressed as the mean  $\pm$  SE of the mean. ND, normal diet (AIN-76); HFD, high-fat diet; Ka, kaempferol; HFD + Ka, high-fat diet + 0.02% kaempferol; H&E, hematoxylin and eosin; TG, triglyceride; FA, fatty acid; FAS, fatty acid synthase; ME, malic enzyme; G6PD, glucose-6-phosphate dehydrogenase; PAP, phosphatidate phosphohydrolase; CPT, carnitine palmitoyltransferase; HMGCR, 3-hydroxy-3-methyl-glutaryl-coenzyme A reductase; ACAT, acyl-coenzyme A:cholesterol acyltransferase; TBARS, thiobarbituric acid reactive substances; MDA, malondialdehyde. Student's *t*-test, \* $P < 0.05$ , \*\* $P < 0.01$ , \*\*\* $P < 0.001$  vs. ND; \* $P < 0.05$ , \*\* $P < 0.01$ , \*\*\* $P < 0.001$  vs. HFD.

(continued to the next page)

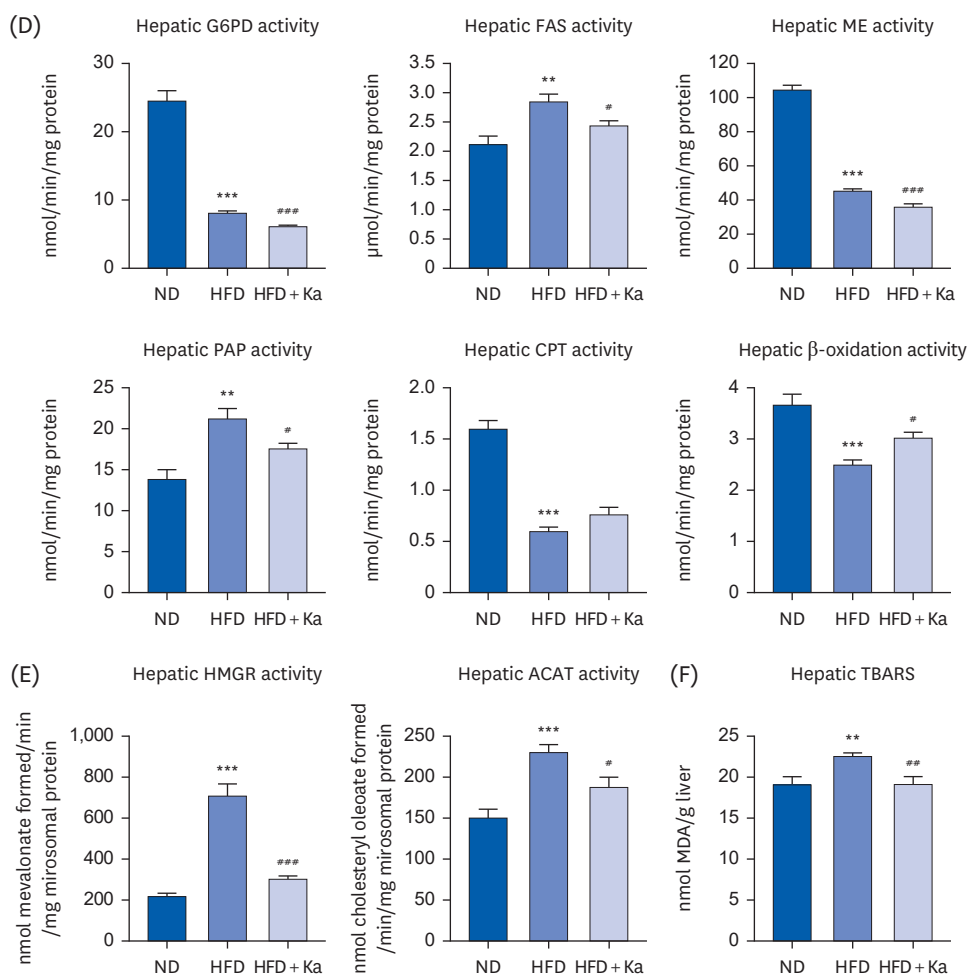


**Fig. 3.** (Continued) Effects of Ka on the liver weight (A), representative images of H&E staining of the liver (B), hepatic lipid profiles (C), hepatic lipid-regulating enzyme activities (D), hepatic cholesterol-regulating enzyme activities (E), and hepatic TBARS (F) in C57BL/6J mice fed a HFD; the data are expressed as the mean  $\pm$  SE of the mean. ND, normal diet (AIN-76); HFD, high-fat diet; Ka, kaempferol; HFD + Ka, high-fat diet + 0.02% kaempferol; H&E, hematoxylin and eosin; TG, triglyceride; FA, fatty acid; FAS, fatty acid synthase; ME, malic enzyme; G6PD, glucose-6-phosphate dehydrogenase; PAP, phosphatidate phosphohydrolase; CPT, carnitine palmitoyltransferase; HMGR, 3-hydroxy-3-methyl-glutaryl-coenzyme A reductase; ACAT, acyl-coenzyme A:cholesterol acyltransferase; TBARS, thiobarbituric acid reactive substances; MDA, malondialdehyde. Student's *t*-test, \**P* < 0.05, \*\**P* < 0.01, \*\*\**P* < 0.001 vs. ND; #*P* < 0.05, ##*P* < 0.01, ###*P* < 0.001 vs. HFD.

Based on the above experimental results, Ka supplementation in high-fat-induced obesity mice is believed to reduce hepatic steatosis and insulin resistance by modulating the activities of hepatic lipid and glucose-regulating enzymes.

### Ka supplementation ameliorated oxidative stress and systemic inflammation, including plasma, liver, and epididymal fat

Chronic obesity increases oxidative stress in the body. The erythrocyte CAT and GSH-Px activities were significantly lower in the HFD group than in the ND group and were increased significantly by Ka supplementation. Accordingly, the level of erythrocyte H<sub>2</sub>O<sub>2</sub> was significantly higher in the HFD group than in the ND group and was decreased by Ka supplementation (Table 3). Unlike circulated antioxidant enzymes, the hepatic SOD and CAT activities were significantly higher in the HFD group than in the ND group. This was attributed to homeostasis to remove ROS generated during the metabolism of excess fat in the liver. Ka supplementation increased the hepatic CAT activity compared to the HFD group, significantly decreasing the mitochondrial H<sub>2</sub>O<sub>2</sub> concentration (Table 3).

Kaempferol mitigates syndrome disease in DIO mice

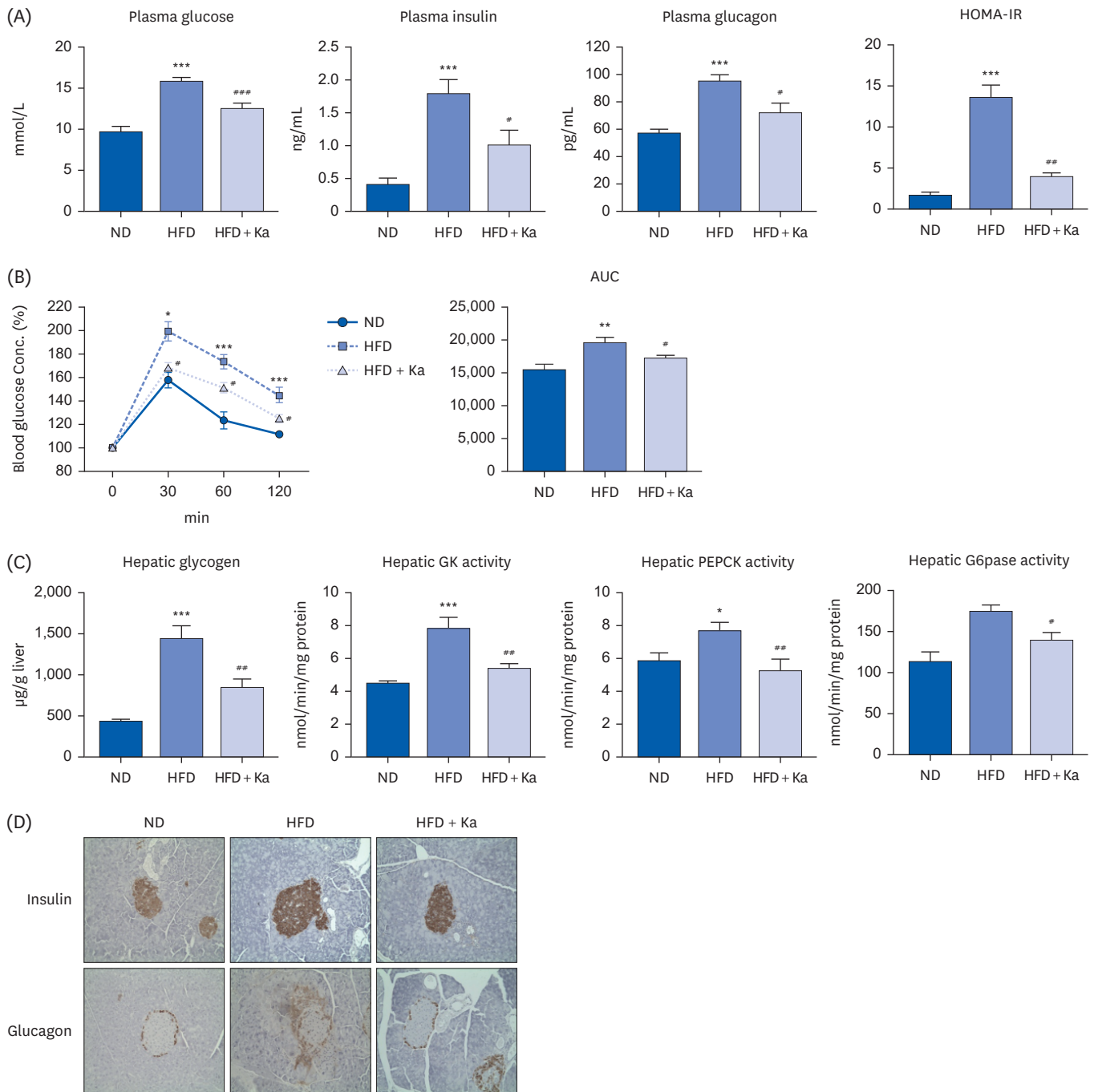


**Fig. 4.** Effects of Ka on the plasma glucose, insulin, glucagon and HOMA-IR (A), IPGTT (B), hepatic glycogen and glucose-regulating enzymes activities (C), representative images for insulin and glucagon of the pancreas (D) in C57BL/6J mice fed a HFD; The data are expressed as the mean ± SE of the mean. ND, normal diet (AIN-76); HFD, high-fat diet; Ka, kaempferol; HFD + Ka, high-fat diet + 0.02% kaempferol; HOMA-IR, homeostatic model assessment of insulin resistance; AUC, area under curve; GK, glucokinase; PEPCK, phosphoenolpyruvate carboxykinase; IPGTT, intraperitoneal glucose tolerance test. Student's *t*-test, \**P* < 0.05, \*\**P* < 0.01, \*\*\**P* < 0.001 vs. ND; #*P* < 0.05, \*\**P* < 0.01, \*\*\**P* < 0.001 vs. HFD.

The level of plasma adiponectin, a hormone specifically expressed and secreted by adipocytes, was significantly lower in the HFD groups than in the ND group and was significantly higher in the Ka group than in the HFD group (Fig. 5A). The plasma levels of leptin and resistin, which are adipokines secreted from adipocytes in obesity or diabetes, were significantly

**Table 3.** Effects of Ka on the antioxidant enzyme activities and H<sub>2</sub>O<sub>2</sub> level of the blood and liver in C57BL/6J mice fed an HFD

Variables	ND	HFD	HFD + Ka
<b>Blood</b>			
SOD (unit/mg Hb)	1.65 ± 0.02	1.71 ± 0.05	1.75 ± 0.04
CAT (μmol/min/mg Hb)	0.228 ± 0.003	0.195 ± 0.005**	0.216 ± 0.002**
GSH-Px (nmol/min/mg Hb)	9.36 ± 0.43	8.14 ± 0.25*	8.41 ± 0.22
Erythrocyte H <sub>2</sub> O <sub>2</sub> (mM/mg Hb)	0.116 ± 0.014	0.148 ± 0.006*	0.130 ± 0.006*
Plasma H <sub>2</sub> O <sub>2</sub> (μM)	60.53 ± 8.45	61.66 ± 9.76	47.24 ± 5.17
<b>Liver</b>			
SOD (unit/mg protein)	93.96 ± 4.71	133.15 ± 3.39***	106.71 ± 3.22***
CAT (μmol/min/mg protein)	0.72 ± 0.03	1.02 ± 0.06*	1.30 ± 0.09*
GSH-Px (nmol/min/mg protein)	10.00 ± 0.18	9.52 ± 0.14	9.87 ± 0.26
Cytosolic H <sub>2</sub> O <sub>2</sub> (μM/mg protein)	7.42 ± 0.50	9.84 ± 0.63*	8.46 ± 0.43
Mitochondrial H <sub>2</sub> O <sub>2</sub> (μM/mg protein)	13.32 ± 0.37	21.69 ± 1.06***	15.15 ± 0.94**

Data are expressed as the mean ±SE of the mean.

ND, normal diet (AIN-76); HFD + Ka, high-fat diet + 0.02% kaempferol; SOD, superoxide dismutase; Hb, hemoglobin; CAT, catalase; GSH-Px, glutathione peroxidase.

Student's *t*-test, \**P* < 0.05, \*\**P* < 0.01, \*\*\**P* < 0.001 vs. ND; \**P* < 0.05, \*\**P* < 0.01, \*\*\**P* < 0.001 vs. HFD.

higher in the HFD group than in the ND group, when Ka was supplemented with an HFD, both adipokine concentrations were significantly lower than that of the HFD group (**Fig. 5A**). The level of adiponectin with a lipolysis inhibitory function was significantly higher in the HFD group than in the ND group and significantly lower in the Ka group than in the HFD group. The PAI-1 level, one of the pro-thrombotic factors, was increased significantly by the intake of a HFD, and no change was observed due to Ka supplementation. The plasma GIP level, which plays a vital role in glucose homeostasis, was significantly higher in the Ka group than in the HFD group (**Fig. 5A**). The levels of pro-inflammatory cytokines/chemokines, such as TNFα, MCP-1, IL-6, and IFN-γ, were suppressed by the Ka treatment relative to that in mice in the HFD group (**Fig. 5B**).

Immunostaining of inflammation markers using CD68 and MCP-1 showed positive staining in the liver and adipocyte tissue in the HFD groups, whereas minor positive staining was observed in the Ka-supplemented group (**Fig. 5C and D**). Tissue fibrosis was assessed using MT staining to display the fibrous tissue of the liver and adipose tissue in the HFD group. The hepatic portal vein of the HFD-fed mice was surrounded by fibrous bands, and epididymal WAT depots in HFD-fed mice contained pronounced trichrome-positive “streaks” interspersed among the adipocytes. The Ka group, however, showed a normal hepatic architecture and fat pad (**Fig. 5C and D**). Microarray analysis of the epididymal WAT also showed that Ka altered the expression of inflammatory response-related genes. Ka supplementation decreased the expression of the inflammatory genes (*Mcp-1*, *Ccl7*, *Ccr5*, *Il7r*, *Ifngr2*, *Cyba*, *Tlr13* and *Rgs1*) and Cd family (*Cd44*, *Cd68*, *Cd72*, *Cd84*, *Cd180*, *Mmp12*, *Prkcb*) (**Supplementary Fig. 1**). The agreement between these biochemical results and mRNA expression results suggests that the anti-obesity effect of Ka supplementation also affects systemic inflammation suppression.

## DISCUSSION

Although the efficacy of Ka has been reported in various physiological effects, such as anti-obesity, anti-inflammatory, anti-diabetic, and antioxidant effects, the controversy surrounding its effectiveness remains [14,15,20,21]. Therefore, this study examined the efficacy of Ka using 3T3-L1 cells and HFD-induced obese mice with dyslipidemia, fatty liver, fibrosis, and IR by controlling inflammation and oxidative stress.

**Kaempferol mitigates syndrome disease in DIO mice**

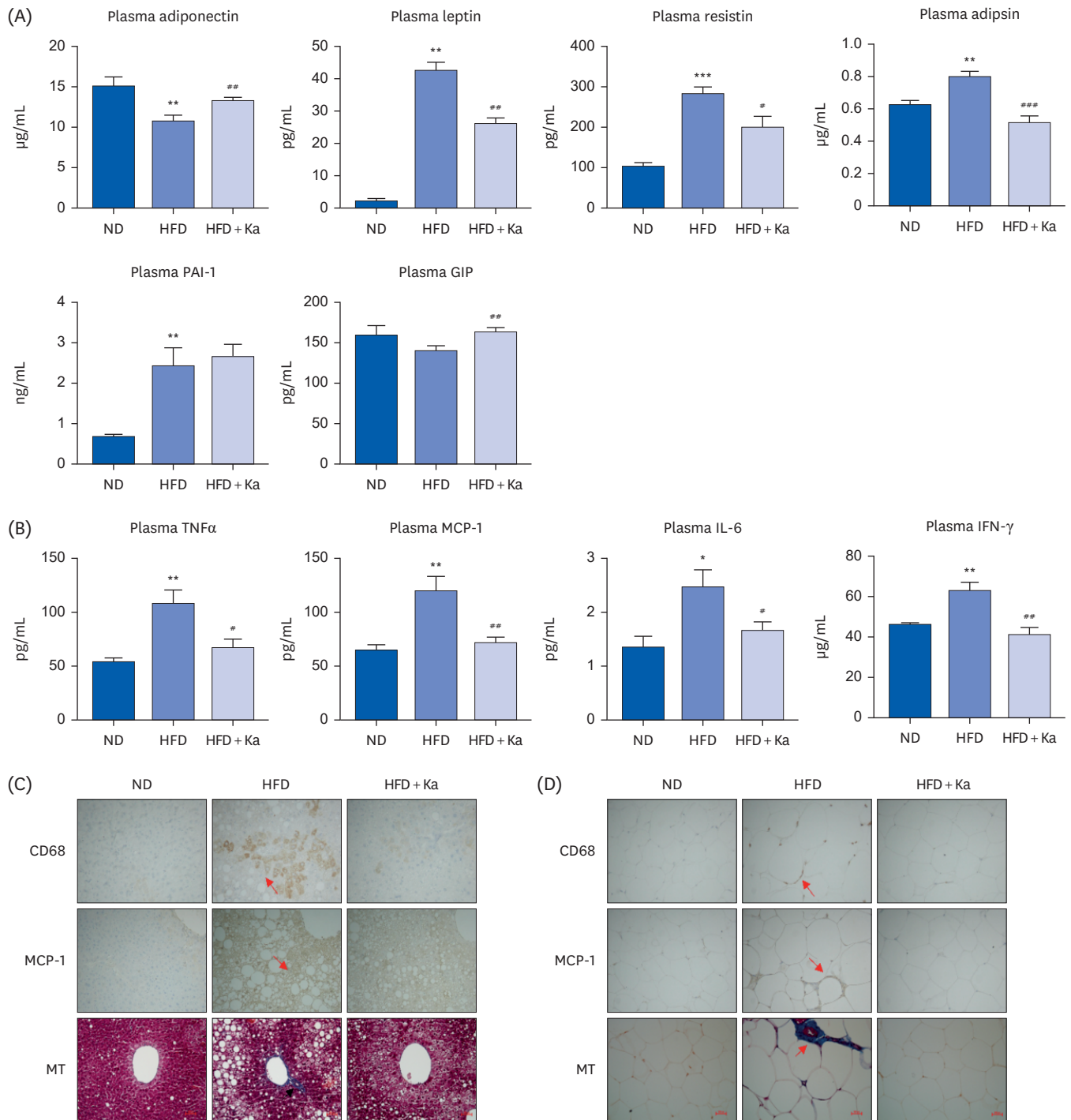


**Fig. 5.** Effects of Ka on adipokines and hormones (A), plasma inflammatory factors (B), representative images of CD68, MCP-1, MT staining of liver (C) and epididymal WAT (D) in C57BL/6J mice fed a HFD; The data are expressed as the mean  $\pm$  SE of the mean. ND, normal diet (AIN-76); HFD, high-fat diet; Ka, kaempferol; HFD + Ka, high-fat diet + 0.02% kaempferol; PAI-1, plasminogen activator inhibitor-1; GIP, gastric inhibitory polypeptide; TNF $\alpha$ , tumor necrosis factor-alpha; MCP-1, monocyte chemoattractant protein-1; IL, interleukin; IFN- $\gamma$ , interferon-gamma; CD, CD molecules; WAT, white adipose tissue. Student's *t*-test, \**P* < 0.05, \*\**P* < 0.01, \*\*\**P* < 0.001 vs. ND; #*P* < 0.05, ##*P* < 0.01, ###*P* < 0.001 vs. HFD.

Torres-Villarreal *et al.* [36] examined the effects of Ka at 60  $\mu$ M over 12 days on regulating the adipogenesis and lipolytic pathways in 3T3-L1 cells. The results showed that the Ka treatment suppressed adipogenesis by 62%. Moreover, in mature adipocytes, Ka led to a 39% decrease

in the accumulation of intracellular lipids. The present study confirmed that treatment with 50  $\mu\text{M}$  Ka for 8 days inhibited lipogenesis in 3T3-L1 cells. In addition, supplementation with Ka reduced body weight starting from the sixth week in high-fat diet-induced obese mice. This weight reduction was attributed to the decrease in WAT weight and adipocyte size, suggesting the efficacy of Ka supplementation in inhibiting lipogenesis.

The body fat mass is closely correlated with metabolic disturbances related to obesity, including insulin resistance, inflammation, and dyslipidemia. The fat stored in adipose tissue is transported to the liver through the plasma non-esterified FAs pool. In the present study, the HFD group had higher plasma and hepatic lipid levels and larger hepatic lipid droplets than the ND group. The Ka supplement decreased the levels of hepatic lipids and plasma TC, phospholipids, ApoB, and AI, as well as hepatic lipid droplet accumulation. These results can occur as part of metabolic syndrome, including obesity, hepatic steatosis, insulin resistance, elevated fasting glucose, and pro-inflammatory states [37]. Insulin signaling plays a crucial role in nutrition and energy balance, and inflammation has been implicated in disrupting the metabolism at various levels [38,39]. In mice models of diet-induced obesity, Ka administration (HFD with 0.1% Ka) has been reported to ameliorate HFD-induced hyperglycemia and inflammation [40]. In the current study, plasma glucose, insulin, glucagon, and HOMA-IR levels were reduced by Ka supplementation, and insulin resistance was also reduced. Furthermore, Ka supplementation regulates the glucose metabolic activity and lipid metabolism in the liver.

Nutritional excess and processing errors can induce stress within organelles, leading to metabolic stress and triggering additional inflammatory pathways [41]. In obesity, the expansion of adipose tissue is widely acknowledged to result in the dysregulated secretion of adipokines and cytokines. Immune mediators, such as TNF $\alpha$ , are believed to play a crucial role in systemic glucose homeostasis by initiating changes that impair insulin effectiveness [42]. Elevated levels of circulating TNF $\alpha$  have been observed in individuals with obesity and nonalcoholic fatty liver disease, with a strong correlation with the severity of liver disease [43,44]. Moreover, the combination of circulating IL-1 $\beta$  and IL-6 levels can predict the onset of type 2 diabetes [45]. In addition, pro-inflammatory cytokines, such as IL-6 and PAI-1, exhibit increased plasma levels in cases of obesity and insulin resistance [46,47]. Interestingly, in the present study, Ka decreased the plasma TNF $\alpha$ , IL-1 $\beta$ , IL-6, and PAI-1 levels significantly, resulting in a reduced inflammatory response, which was associated with a noticeable improvement in adiposity, insulin resistance, and hepatic steatosis induced by Ka.

TNF $\alpha$  and IL-6 have also been implicated in hepatic tissue fibrosis because they promote the transition of hepatic stellate cells into myofibroblasts. In addition, they have the potential to induce fibrosis within WAT [48,49]. This study confirmed the occurrence of inflammation and fibrosis in the HFD group, but supplementation with Ka during the HFD almost eliminated these phenomena. Therefore, the reduction in plasma TNF $\alpha$  and IL-6 concentrations due to Ka supplementation helps inhibit the fibrotic responses. The administration of TNF $\alpha$  and IL-6 to mice enhances MCP-1 production in reaction to oxidized LDL. Moreover, heightened TNF $\alpha$  and IL-6 expression correlates with the increased expression of the scavenger receptor CD68. Thus, MCP-1 and CD68 exhibit heightened expression in response to inflammatory stimuli [50]. In this experiment, the MCP-1 concentration was decreased significantly in the plasma. Furthermore, the protein expression of CD68 and MCP-1 in the liver and adipose tissue was almost negligible in the Ka group, while it was significant in the HFD group. The microarray results of WAT suggest that



inflammation-related genes were also decreased by Ka supplementation. This is consistent with previous research findings [48,49].

Several studies have reported that excessive generation of ROS due to obesity or excessive adipose tissue leads to systemic metabolic disorders such as insulin resistance [11]. The main mechanisms of the endogenous antioxidant defense system include the following: SOD facilitates the conversion of superoxide anions, produced as byproducts within cells, into  $H_2O_2$ . Subsequently,  $H_2O_2$  is reduced to  $H_2O$  by the actions of GSH-Px and CAT. In essence, SOD acts as a primary cellular protector by eliminating superoxide anions and protecting cells from oxidative stress. In high-fat diet-induced obese mice, supplementation with Ka led to a significant increase in CAT activity and a decrease in  $H_2O_2$  content in the blood and liver.

These findings suggest that Ka supplementation ameliorates obesity, fatty liver, and insulin resistance in HFD-induced obese mice. The anti-diabetic effect of Ka is related to the improvements in hyperglycemia, glucose-regulating hormone levels, and the HOMA-IR value. Ka also alleviates nonalcoholic fatty liver disease by regulating the hepatic lipid-regulating enzyme activities and decreasing lipid droplets. In addition, the anti-obesity effect of Ka is closely related to its anti-inflammatory effect and decreased adipokine secretion and fibrosis accumulation in WAT and the liver. Overall, these findings indicate that Ka may be beneficial for preventing diet-induced obesity, inflammation, and diabetes. The increase in inflammation and oxidative stress related to obesity contributes to insulin resistance and hepatic steatosis [51]. This pathway worsens obesity and creates a vicious cycle. Therefore, additional research will be needed to determine how Ka exhibits its efficacy through specific molecules or mechanisms, breaking this vicious cycle.

## SUPPLEMENTARY MATERIAL

### Supplementary Fig. 1

Effects of Ka on the expression of inflammatory response-related genes of epididymal WAT in C57BL/6J mice fed a HFD; The data are expressed as the mean  $\pm$  SE of the mean.

## REFERENCES

1. Ng M, Fleming T, Robinson M, Thomson B, Graetz N, Margono C, Mullany EC, Biryukov S, Abbafati C, Abera SE, et al. Global, regional, and national prevalence of overweight and obesity in children and adults during 1980-2013: a systematic analysis for the Global Burden of Disease Study 2013. *Lancet* 2014;384:766-81. [PUBMED](#) | [CROSSREF](#)
2. Fried SK, Bunkin DA, Greenberg AS. Omental and subcutaneous adipose tissues of obese subjects release interleukin-6: depot difference and regulation by glucocorticoid. *J Clin Endocrinol Metab* 1998;83:847-50. [PUBMED](#) | [CROSSREF](#)
3. Shimomura I, Funahashi T, Takahashi M, Maeda K, Kotani K, Nakamura T, Yamashita S, Miura M, Fukuda Y, Takemura K, et al. Enhanced expression of PAI-1 in visceral fat: possible contributor to vascular disease in obesity. *Nat Med* 1996;2:800-3. [PUBMED](#) | [CROSSREF](#)
4. Steppan CM, Bailey ST, Bhat S, Brown EJ, Banerjee RR, Wright CM, Patel HR, Ahima RS, Lazar MA. The hormone resistin links obesity to diabetes. *Nature* 2001;409:307-12. [PUBMED](#) | [CROSSREF](#)
5. Kahn BB, Flier JS. Obesity and insulin resistance. *J Clin Invest* 2000;106:473-81. [PUBMED](#) | [CROSSREF](#)
6. Shoelson SE, Herrero L, Naaz A. Obesity, inflammation, and insulin resistance. *Gastroenterology* 2007;132:2169-80. [PUBMED](#) | [CROSSREF](#)

7. Huang Cao ZF, Stoffel E, Cohen P. Role of perivascular adipose tissue in vascular physiology and pathology. *Hypertension* 2017;69:770-7. [PUBMED](#) | [CROSSREF](#)
8. Reho JJ, Rahmouni K. Oxidative and inflammatory signals in obesity-associated vascular abnormalities. *Clin Sci (Lond)* 2017;131:1689-700. [PUBMED](#) | [CROSSREF](#)
9. Shah S, Iqbal M, Karam J, Salifu M, McFarlane SI. Oxidative stress, glucose metabolism, and the prevention of type 2 diabetes: pathophysiological insights. *Antioxid Redox Signal* 2007;9:911-29. [PUBMED](#) | [CROSSREF](#)
10. Park K, Gross M, Lee DH, Holvoet P, Himes JH, Shikany JM, Jacobs DR Jr. Oxidative stress and insulin resistance: the coronary artery risk development in young adults study. *Diabetes Care* 2009;32:1302-7. [PUBMED](#) | [CROSSREF](#)
11. Jakubiak GK, Osadnik K, Lejawa M, Osadnik T, Gołowski M, Lewandowski P, Pawlas N. "Obesity and insulin resistance" is the component of the metabolic syndrome most strongly associated with oxidative stress. *Antioxidants (Basel)* 2021;11:79. [PUBMED](#) | [CROSSREF](#)
12. An G, Gallegos J, Morris ME. The bioflavonoid kaempferol is an Abcg2 substrate and inhibits Abcg2-mediated quercetin efflux. *Drug Metab Dispos* 2011;39:426-32. [PUBMED](#) | [CROSSREF](#)
13. Häkkinen SH, Kärenlampi SO, Heinonen IM, Mykkänen HM, Törrönen AR. Content of the flavonols quercetin, myricetin, and kaempferol in 25 edible berries. *J Agric Food Chem* 1999;47:2274-9. [PUBMED](#) | [CROSSREF](#)
14. da-Silva WS, Harney JW, Kim BW, Li J, Bianco SD, Crescenzi A, Christoffolete MA, Huang SA, Bianco AC. The small polyphenolic molecule kaempferol increases cellular energy expenditure and thyroid hormone activation. *Diabetes* 2007;56:767-76. [PUBMED](#) | [CROSSREF](#)
15. Yu SF, Shun CT, Chen TM, Chen YH. 3-O-β-D-glucosyl-(1→6)-β-D-glucosyl-kaempferol isolated from *Sauropus androgenus* reduces body weight gain in Wistar rats. *Biol Pharm Bull* 2006;29:2510-3. [PUBMED](#) | [CROSSREF](#)
16. Lee YJ, Suh KS, Choi MC, Chon S, Oh S, Woo JT, Kim SW, Kim JW, Kim YS. Kaempferol protects HIT-T15 pancreatic beta cells from 2-deoxy-D-ribose-induced oxidative damage. *Phytother Res* 2010;24:419-23. [PUBMED](#) | [CROSSREF](#)
17. Suh KS, Choi EM, Kwon M, Chon S, Oh S, Woo JT, Kim SW, Kim JW, Kim YS. Kaempferol attenuates 2-deoxy-D-ribose-induced oxidative cell damage in MC3T3-E1 osteoblastic cells. *Biol Pharm Bull* 2009;32:746-9. [PUBMED](#) | [CROSSREF](#)
18. Crespo I, García-Mediavilla MV, Gutiérrez B, Sánchez-Campos S, Tuñón MJ, González-Gallego J. A comparison of the effects of kaempferol and quercetin on cytokine-induced pro-inflammatory status of cultured human endothelial cells. *Br J Nutr* 2008;100:968-76. [PUBMED](#) | [CROSSREF](#)
19. Hämäläinen M, Nieminen R, Vuorela P, Heinonen M, Moilanen E. Anti-inflammatory effects of flavonoids: genistein, kaempferol, quercetin, and daidzein inhibit STAT-1 and NF-κB activations, whereas flavone, isorhamnetin, naringenin, and pelargonidin inhibit only NF-κB activation along with their inhibitory effect on iNOS expression and NO production in activated macrophages. *Mediators Inflamm* 2007;2007:45673. [PUBMED](#) | [CROSSREF](#)
20. Ninomiya K, Matsuda H, Kubo M, Morikawa T, Nishida N, Yoshikawa M. Potent anti-obese principle from *Rosa canina*: structural requirements and mode of action of trans-tilliroside. *Bioorg Med Chem Lett* 2007;17:3059-64. [PUBMED](#) | [CROSSREF](#)
21. Christensen KB, Petersen RK, Kristiansen K, Christensen LP. Identification of bioactive compounds from flowers of black elder (*Sambucus nigra* L.) that activate the human peroxisome proliferator-activated receptor (PPAR) γ. *Phytother Res* 2010;24 Suppl 2:S129-32. [PUBMED](#) | [CROSSREF](#)
22. Carroll NV, Longley RW, Roe JH. The determination of glycogen in liver and muscle by use of anthrone reagent. *J Biol Chem* 1956;220:583-93. [PUBMED](#) | [CROSSREF](#)
23. Davidson AL, Arion WJ. Factors underlying significant underestimations of glucokinase activity in crude liver extracts: physiological implications of higher cellular activity. *Arch Biochem Biophys* 1987;253:156-67. [PUBMED](#) | [CROSSREF](#)
24. Bentle LA, Lardy HA. Interaction of anions and divalent metal ions with phosphoenolpyruvate carboxykinase. *J Biol Chem* 1976;251:2916-21. [PUBMED](#) | [CROSSREF](#)
25. Alegre M, Ciudad CJ, Fillat C, Guinovart JJ. Determination of glucose-6-phosphatase activity using the glucose dehydrogenase-coupled reaction. *Anal Biochem* 1988;173:185-9. [PUBMED](#) | [CROSSREF](#)
26. Nepokroeff CM, Lakshmanan MR, Porter JW. Fatty-acid synthase from rat liver. *Methods Enzymol* 1975;35:37-44. [PUBMED](#) | [CROSSREF](#)
27. Pitkänen E, Pitkänen O, Uotila L. Enzymatic determination of unbound D-mannose in serum. *Eur J Clin Chem Clin Biochem* 1997;35:761-6. [PUBMED](#) | [CROSSREF](#)

28. Markwell MA, McGroarty EJ, Bieber LL, Tolbert NE. The subcellular distribution of carnitine acyltransferases in mammalian liver and kidney. A new peroxisomal enzyme. *J Biol Chem* 1973;248:3426-32. [PUBMED](#) | [CROSSREF](#)
29. Lazarow PB. Assay of peroxisomal beta-oxidation of fatty acids. *Methods Enzymol* 1981;72:315-9. [PUBMED](#) | [CROSSREF](#)
30. Shapiro DJ, Nordstrom JL, Mitschelen JJ, Rodwell VW, Schimke RT. Micro assay for 3-hydroxy-3-methylglutaryl-CoA reductase in rat liver and in L-cell fibroblasts. *Biochim Biophys Acta* 1974;370:369-77. [PUBMED](#) | [CROSSREF](#)
31. Gillies PJ, Rathgeb KA, Perri MA, Robinson CS. Regulation of acyl-CoA:cholesterol acyltransferase activity in normal and atherosclerotic rabbit aortas: role of a cholesterol substrate pool. *Exp Mol Pathol* 1986;44:329-39. [PUBMED](#) | [CROSSREF](#)
32. Ohkawa H, Ohishi N, Yagi K. Assay for lipid peroxides in animal tissues by thiobarbituric acid reaction. *Anal Biochem* 1979;95:351-8. [PUBMED](#) | [CROSSREF](#)
33. Marklund S, Marklund G. Involvement of the superoxide anion radical in the autoxidation of pyrogallol and a convenient assay for superoxide dismutase. *Eur J Biochem* 1974;47:469-74. [PUBMED](#) | [CROSSREF](#)
34. Aebi H. Catalase *in vitro*. *Methods Enzymol* 1984;105:121-6. [PUBMED](#) | [CROSSREF](#)
35. Paglia DE, Valentine WN. Studies on the quantitative and qualitative characterization of erythrocyte glutathione peroxidase. *J Lab Clin Med* 1967;70:158-69. [PUBMED](#)
36. Torres-Villarreal D, Camacho A, Castro H, Ortiz-Lopez R, de la Garza AL. Anti-obesity effects of kaempferol by inhibiting adipogenesis and increasing lipolysis in 3T3-L1 cells. *J Physiol Biochem* 2019;75:83-8. [PUBMED](#) | [CROSSREF](#)
37. Aguilera CM, Gil-Campos M, Cañete R, Gil A. Alterations in plasma and tissue lipids associated with obesity and metabolic syndrome. *Clin Sci (Lond)* 2008;114:183-93. [PUBMED](#) | [CROSSREF](#)
38. Pradhan A. Obesity, metabolic syndrome, and type 2 diabetes: inflammatory basis of glucose metabolic disorders. *Nutr Rev* 2007;65:S152-6. [PUBMED](#) | [CROSSREF](#)
39. Saltiel AR, Olefsky JM. Inflammatory mechanisms linking obesity and metabolic disease. *J Clin Invest* 2017;127:1-4. [PUBMED](#) | [CROSSREF](#)
40. Bian Y, Lei J, Zhong J, Wang B, Wan Y, Li J, Liao C, He Y, Liu Z, Ito K, et al. Kaempferol reduces obesity, prevents intestinal inflammation, and modulates gut microbiota in high-fat diet mice. *J Nutr Biochem* 2022;99:108840. [PUBMED](#) | [CROSSREF](#)
41. Nainu F, Frediansyah A, Mamada SS, Permana AD, Salampe M, Chandran D, Emran TB, Simal-Gandara J. Natural products targeting inflammation-related metabolic disorders: a comprehensive review. *Heliyon* 2023;9:e16919. [PUBMED](#) | [CROSSREF](#)
42. Picchi A, Gao X, Belmadani S, Potter BJ, Focardi M, Chilian WM, Zhang C. Tumor necrosis factor-alpha induces endothelial dysfunction in the prediabetic metabolic syndrome. *Circ Res* 2006;99:69-77. [PUBMED](#) | [CROSSREF](#)
43. Garcia-Ruiz I, Rodríguez-Juan C, Díaz-Sanjuan T, del Hoyo P, Colina F, Muñoz-Yagüe T, Solís-Herruzo JA. Uric acid and anti-TNF antibody improve mitochondrial dysfunction in ob/ob mice. *Hepatology* 2006;44:581-91. [PUBMED](#) | [CROSSREF](#)
44. McCullough AJ. Pathophysiology of nonalcoholic steatohepatitis. *J Clin Gastroenterol* 2006;40 Suppl 1:S17-29. [PUBMED](#)
45. Spranger J, Kroke A, Möhlig M, Hoffmann K, Bergmann MM, Ristow M, Boeing H, Pfeiffer AF. Inflammatory cytokines and the risk to develop type 2 diabetes: results of the prospective population-based European Prospective Investigation into Cancer and Nutrition (EPIC)-Potsdam Study. *Diabetes* 2003;52:812-7. [PUBMED](#) | [CROSSREF](#)
46. Bastard JP, Maachi M, Van Nhieu JT, Jardel C, Bruckert E, Grimaldi A, Robert JJ, Capeau J, Hainque B. Adipose tissue IL-6 content correlates with resistance to insulin activation of glucose uptake both *in vivo* and *in vitro*. *J Clin Endocrinol Metab* 2002;87:2084-9. [PUBMED](#) | [CROSSREF](#)
47. Juhan-Vague I, Alessi MC, Mavri A, Morange PE. Plasminogen activator inhibitor-1, inflammation, obesity, insulin resistance and vascular risk. *J Thromb Haemost* 2003;1:1575-9. [PUBMED](#) | [CROSSREF](#)
48. Tarrats N, Moles A, Morales A, Garcia-Ruiz C, Fernández-Checa JC, Mari M. Critical role of tumor necrosis factor receptor 1, but not 2, in hepatic stellate cell proliferation, extracellular matrix remodeling, and liver fibrogenesis. *Hepatology* 2011;54:319-27. [PUBMED](#) | [CROSSREF](#)
49. Martin S, Fernandez-Rojo MA, Stanley AC, Bastiani M, Okano S, Nixon SJ, Thomas G, Stow JL, Parton RG. Caveolin-1 deficiency leads to increased susceptibility to cell death and fibrosis in white adipose tissue: characterization of a lipodystrophic model. *PLoS One* 2012;7:e46242. [PUBMED](#) | [CROSSREF](#)

50. Arfian N, Setyaningsih WA, Romi MM, Sari DC. Heparanase upregulation from adipocyte associates with inflammation and endothelial injury in diabetic condition. BMC Proc 2019;13:17. [PUBMED](#) | [CROSSREF](#)
51. Chawla A, Nguyen KD, Goh YP. Macrophage-mediated inflammation in metabolic disease. Nat Rev Immunol 2011;11:738-49. [PUBMED](#) | [CROSSREF](#)